

## SEISMIC LOSS ASSESSMENT CONSIDERING LOW-DAMAGE REPAIR OF NON-STRUCTURAL COMPONENTS

M.J. Fox<sup>1</sup>, T.Z. Yeow<sup>2</sup> & G.J. O'Reilly<sup>3</sup>

<sup>1</sup>Guy Carpenter, Milan, Italy, [matthew-james.fox@guycarp.com](mailto:matthew-james.fox@guycarp.com)

<sup>2</sup> University of Tokyo, Tokyo, Japan

<sup>3</sup> IUSS Pavia, Pavia, Italy

**Abstract:** *Seismic loss assessment is a powerful tool for understanding potential losses in future earthquakes and supporting decision-making in the design of new buildings or retrofit of existing ones. Following the methodology of FEMA P-58, annualised economic losses can be calculated, but on the basis that the building's seismic vulnerability does not change with time. This does not reflect the reality of many real-world cases where owners have opted to replace earthquake damaged building components with new low-damage solutions. In this work, seismic loss assessment is carried out using a novel approach that simulates sets of earthquakes over the anticipated life of the building. Considering all events in sequence, the building model can be updated to reflect changes that might be made post-earthquake or simply through elective interventions. Losses are calculated for an example 12-storey steel moment resisting frame building, hypothetically located in Wellington, New Zealand, assuming that severely damaged non-structural components are replaced with new low-damage components following each event. Different configurations of non-structural components are considered, along with different assumptions on how damaged components are repaired following an event. It is shown that for buildings with very fragile non-structural components, assumptions on the post-earthquake repair of non-structural components can have a notable effect on the expected annual loss parameter. This is important when considering cost-benefit analyses for making decisions on retrofitting non-structural components in existing buildings.*

### 1. Introduction

Traditionally, the primary objective for the seismic design of structures has been to prevent loss of life or serious injury during strong earthquakes. However, starting from around the early '90s, this primary focus on life safety was challenged, and further consideration was also given to reducing economic losses and post-earthquake functionality. The major catalyst for this change was arguably the 1989 Loma Prieta and 1994 Northridge earthquakes. Both of these events struck close to populated areas and, while resulting in fewer than 100 deaths (Hamburger, 1996), they caused significant economic losses and disruption, with Northridge at the time being the most expensive natural disaster in history. Similar observations have been made in other parts of the world, such as New Zealand, where the 2011 Christchurch earthquake resulted in significant economic losses relative to the fairly limited loss of life.

The desire to design structures that target specific performance objectives rather than following more prescriptive approaches led to the rise of Performance-Based Earthquake Engineering (PBEE). Although contributions to PBEE have come from many different organisations around the globe, the most widely

recognised methodology is that of the Pacific Earthquake Engineering Research (PEER) centre. The PEER PBEE methodology was formalised in FEMA P-58, and supporting tools were developed to allow researchers and practitioners to perform seismic loss assessments for buildings. Seismic loss assessment allows engineers to evaluate a range of performance metrics related to life safety, repair costs, repair time and, more recently, environmental impacts. One of the most popular metrics is Expected Annual Loss (EAL), usually characterised by the direct economic losses associated with the repair costs for each damaged element in the building.

EAL can be used, for example, to compare the relative performance of two different structural systems for a proposed new building and help guide decision-makers in their choices. Similarly, EAL can be used in a cost-benefit analysis to explore whether the upfront cost of seismically retrofitting a structure will likely be recovered within a specific time frame (e.g. Sousa and Monteiro, 2018). In this latter case, one issue in applying the approach of FEMA P-58 is that it cannot account for changes in the state of the building following individual events. For example, an owner may choose after an event to “build back better” and replace a severely damaged building component with a more resilient equivalent.

The effect of post-earthquake resilience improvements on calculated losses is the subject of the current paper. This is examined through the analysis of a case-study building by assuming that severely damaged non-structural components are not repaired to their pre-earthquake condition but instead replaced with a “low-damage”, i.e., more resilient equivalent. The following sections describe the new loss-assessment methodology that has been adopted, a description of the case-study building, analysis of the results and, finally, conclusions.

## 2. Loss assessment methodology

To consider the effects of low-damage repair of non-structural components, a new loss assessment methodology needed to be formulated. This was based on the existing FEMA P-58 approach, which is outlined in the following section, along with limitations relevant to the current research. A description of the modified approach then follows.

### 2.1. FEMA P-58

The most established approach to seismic loss assessment is the so-called PEER methodology, which is formalised in FEMA P-58. Losses are calculated on a component-by-component basis and the overall methodology comprises the four key steps of: (i) hazard analysis to obtain the rate of exceedance of a given intensity of earthquake ground shaking ( $\lambda_{IM}$ ), (ii) structural analysis to obtain engineering demand parameters (EDP) given an intensity of shaking ( $f[EDP|IM]$ ), (iii) damage analysis to obtain the damage state of a component (DS) given EDP ( $f[DS|EDP]$ ), and (iv) loss analysis to obtain repair cost (\$Loss) given DS ( $P[\$Loss|DS]$ ). Loss calculations can be intensity-based, scenario-based or time-based. In the current work, it is the time-based calculation that is of interest, i.e. the analyst would like to know what the losses might be over a given period of time. As mentioned previously, the most commonly utilised metric is EAL, which can be calculated by applying the total probability theorem and solving the multi-level integral of Equation 1:

$$EAL = \iiint P[\$Loss|DS]f[DS|EDP]f[EDP|IM]|d\lambda_{IM}(im)|dEDPdDS \quad (1)$$

In practice, Equation 1 is solved numerically via Monte Carlo simulation, for example, using the PACT software that accompanies FEMA P-58. The key limitation, with respect to the objectives of the current work, is that the building is effectively time-invariant, i.e. it is assumed that following an earthquake, the building is returned exactly to its pre-earthquake state. This is problematic when degradation or accumulation of damage needs to be taken into consideration (e.g. Iervolino *et al.*, 2016). It is also potentially problematic when evaluating existing buildings that have not been designed or detailed following modern practices or code requirements. This is because when such buildings are damaged during an earthquake, it is likely that any repairs or replacement of components will aim to achieve improved performance (e.g. in line with code requirements or construction practices).

### 2.2. Modified loss assessment formulation

To account for the change in the building’s state following a damaging earthquake, the approach for FEMA P-58 has been modified to allow for updating of the building component inventory post event. The modified approach follows the steps below:

1. Perform probabilistic seismic hazard analysis (PSHA) to obtain the hazard curve for the site in terms of a suitable intensity measure (IM).
2. Perform structural analysis to obtain the distribution of EDPs at a set of relevant intensities and the corresponding collapse fragility curve. A popular option for this step is multiple-stripe analysis or MSA (Jalayer and Cornell, 2009), which utilises nonlinear time-history analysis with different sets of ground motions at a chosen number of intensities.
3. Populate a building component inventory, which comprises the number and location of all damageable components within the building. Each component is characterised by fragility curves for a number of damage states and corresponding repair costs.
4. Using the hazard curve obtained in step one, simulate a random set of earthquakes, or more correctly earthquake intensities, over the desired time period (e.g. 50 years).
5. For the first simulated earthquake in the set, generate a corresponding vector of EDPs. This can be achieved using the MSA results from Step 2 and Appendix G of FEMA P-58, which simulates a vector of EDPs based on limited analyses. In the (likely) case that the simulated earthquake intensity does not align with one of the intensities considered in the MSA, linear interpolation (of the mean EDP vector and covariance matrix) can be used.
6. Calculate a single loss realisation for the simulated earthquake following the same methodology utilised in FEMA P-58 and the associated PACT software (in PACT, a large number of realisations are generated as part of the Monte Carlo method).
7. Record the loss from the simulated earthquake and update the building inventory model as required. In the current work, this means replacing, as desired, damaged components with new low-damage components.
8. Repeat steps 5-7 for all simulated earthquakes in the set.
9. Repeat steps 4-8 for a large number of trials.

Several important observations can be made regarding the above procedure. The first is that although the component inventory can be updated post-earthquake, the structural analysis results cannot. This means that the approach is not suitable for analysing buildings that are likely to experience major changes in structural response. However, this could be accounted for by performing structural analysis on different levels of pre-damaged structures and updating the structural response (at Step 5) as required. Similarly, it is assumed that any modification in the non-structural component part of the damageable inventory used in loss assessment will also not impact the structural response. The second is that many simulated losses will correspond to low-intensity earthquakes while only a few will correspond to high-intensity earthquakes (by comparison, PACT generates the same number of realisations at each intensity). This is reasonable given that, in the real world, lower-intensity earthquakes occur much more frequently than high-intensity earthquakes. However, it could result in an unnecessarily large amount of analysis at low intensities, making the process somewhat cumbersome to implement. The third is that the newly formulated approach is substantially more computationally expensive than the FEMA P-58 methodology. However, the overall computation time for steps 4-9 is still relatively low (in the order of 5 minutes for 1000 trials of 50 years with the case study building, discussed in the next section).

### 3. Case-study building

#### 3.1. Structural overview

The case-study building that is to be investigated is a 12-storey steel frame building hypothetically located in Wellington, New Zealand. The building was previously examined in loss-assessment studies by Yeow *et al.* (2018) and relies on steel moment-resisting frames with reduced beam section connections as the lateral load-resisting system in both orthogonal directions. Design of the structural system was undertaken in accordance with the New Zealand steel structures standard NZS3404 (SNZ, 1997) for the seismic actions specified in the New Zealand design actions standard NZS1170.5 (SNZ, 2004).

Class C (i.e. shallow) subsoils were assumed for the hypothetical site, and the building was designed for Importance Level 2. An iterative design approach was adopted to obtain the lightest frame design possible whilst remaining compliant with the aforementioned standards. However, to keep the design simple, beam section sizes were generally only varied every three storeys. The fundamental period of the building was calculated to be 2.9 s, and the corresponding (elastic) design spectral acceleration for the 500-year return

period used in the design of IL2 structures was  $Sa(2.9) = 0.40$  g. The design was governed by the NZS1170.5 drift limit of 2.5% at the ultimate limit state (ULS).

The designed structure was analysed using MSA to obtain the storey drifts and total floor acceleration distributions and the collapse fragility. The structural model was developed in Ruaumoko2D (Carr, 2004) and analysed at the eight intensities shown in Figure 1(a). Sets of 20 ground motions were used at each intensity and selection and scaling was performed using the generalised conditional intensity measure approach (Bradley, 2010; Bradley, 2012) with  $Sa(2.0)$  as the conditioning intensity measure. The structural analysis results in terms of peak storey drift are shown in Figure 1(b), along with the collapse fragility curve in Figure 1(c). For further details, the reader is referred to Yeow et al. (2018).

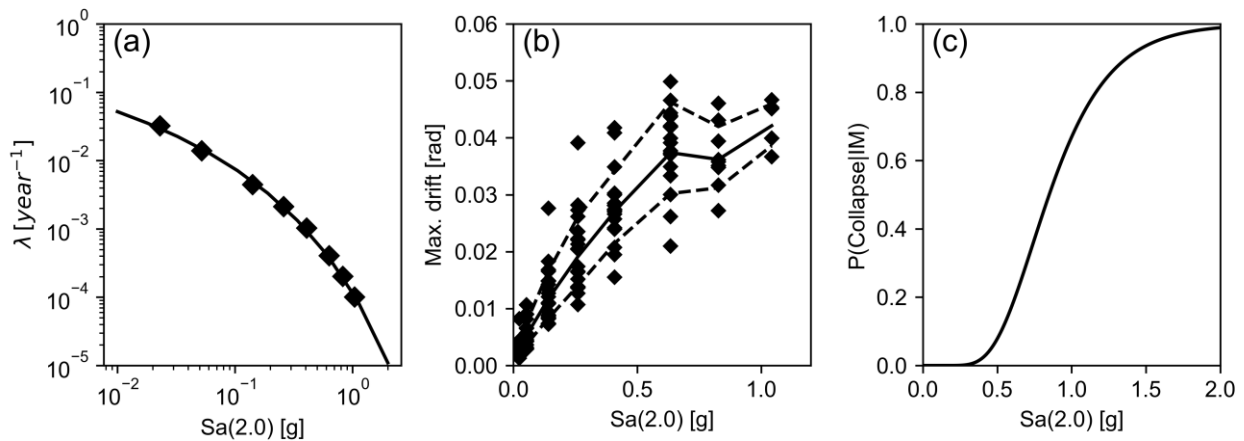


Figure 1. (a) Site hazard curve and intensities used in MSA. (b) Maximum drifts from structural analysis. (c) Collapse fragility curve.

### 3.2. Non-structural inventory

The building's non-structural fit-out was again based on the work of Yeow et al. (2018); however, the specific components were chosen to be more vulnerable. In this way, the building represents a structure designed to modern standards but without specific attention given to the seismic protection of non-structural components (and thus a potential candidate for non-structural retrofit). Although the building is hypothetically located in New Zealand, the non-structural components – along with corresponding fragilities and consequence functions – were generally taken directly from the FEMA P-58 database. This choice was made so that all the work was undertaken with a well-established database; however, it is worth noting that New Zealand-specific non-structural fragilities and consequence functions are available (e.g. Yeow et al., 2018b; Fox et al., 2024).

For each “vulnerable” component in the “as-built” structure, an equivalent low-damage component was selected. For example, Figure 2 shows the chosen fragility functions for full-height steel stud partition walls, which are based on the results reported by Retemales et al. (2013). In this case, for each of the three damage states, the median ( $\theta$ ) of the lognormal curve corresponds to a 1% larger inter-storey drift ratio (IDR) whilst the dispersion ( $\beta$ ) remains unchanged.

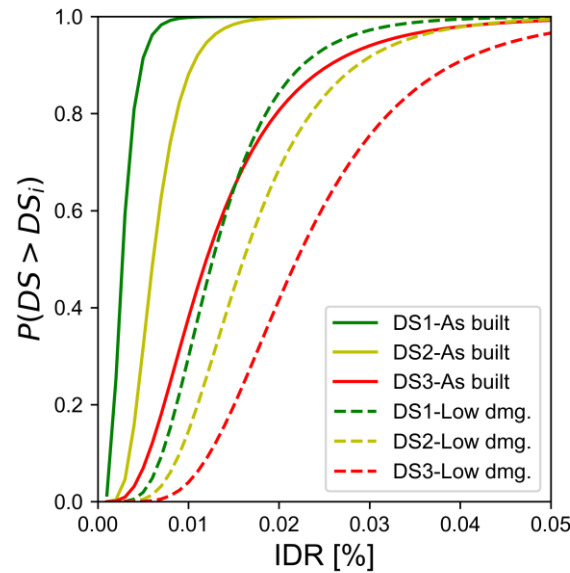


Figure 2. As-built and low-damage fragility curves for full-height partition walls.

Table 1 lists the location and quantity of non-structural components assumed for the building fit-out. The fragility functions for all components and source references are provided in Table A1.

Table 1. List of damageable structural and non-structural components

Component name	Location	Quantity
Steel column base plates	Ground level	10
RBS connection, one-sided, small section	Levels 10 to 12	4 per floor
RBS connection, one-sided, large section	Levels 1 to 9	4 per floor
RBS connection, two-sided, small section	Levels 10 to 12	6 per floor
RBS connection, two-sided, large section	Levels 1 to 9	6 per floor
External cladding	All floor levels	555 m <sup>2</sup> per floor
Internal glass partitions	All floor levels	89 m <sup>2</sup> per floor
Full-height steel stud partition walls	All floor levels	88 m <sup>2</sup> per floor
Partial-height steel stud partition walls	All floor levels	94 m <sup>2</sup> per floor
Precast concrete stairs	All floor levels	1
Suspended ceiling	All floor levels	1235 m <sup>2</sup> per floor
Traction elevator	All floor levels	3
Potable water piping	All floor levels	610 m per floor
Sanitary waste piping	All floor levels	305 m per floor
Chiller	Ground floor	1
Cooling tower	Roof	1
HVAC in-line fan	All floor levels	80 per floor
HVAC ducting	All floor levels	610 m per floor
HVAC drops/diffusers	All floor levels	150 per floor
Variable air volume (VAV) box	All floor levels	30 per floor
Fire sprinkler water piping	All floor levels	915 m per floor
Fire sprinkler drop	All floor levels	400 per floor
Transformer	Ground floor	1
Air handling unit	Roof	1

#### 4. Loss assessment and results

To investigate the impact that post-earthquake repair strategies have on direct economic losses, the case-study building was analysed using the approach described in Section 2. Two different scenarios were

considered: (i) the case conventionally assumed for loss assessment where earthquake-damaged components are repaired to their pre-earthquake condition or replaced with identical components (herein referred to as the benchmark), and (ii) the case where severely damaged components (i.e. requiring replacement) are replaced with low-damage equivalent components.

To simplify the analyses, it was assumed that there was no difference in cost to replace a component with a conventional or low-damage component. Analyses were performed for a period of 50 years, a common value used for the design life of new buildings, and 10,000 trials were performed.

#### **4.1. Results for individual 50-year periods**

Although the key results of interest are those pertaining to a large number of trials, it is helpful to also look at the outcomes of several 50-year periods individually. Figure 3 shows the cumulative losses from four different 50-year periods for both scenarios, along with the intensity of earthquakes occurring in each period. In the first case (Figure 3(a)), there is a strong earthquake causing significant damage after 5 years, but then after that, there is only one more very weak earthquake, which does not cause significant damage. Although the first earthquake causes sufficient damage for some components to be replaced with new low-damage equivalents, there are no further damaging earthquakes in the time period and so there is no difference between the benchmark and low-damage cases. In the second case (Figure 3(b)), there is a minor earthquake after 11 years, which causes minor damage that only requires minor repairs and not the replacement of components. Therefore, when a second stronger quake occurs, the benchmark and low-damage cases give the same result. The third case (Figure 3(c)) is similar, with several weak to moderate earthquakes, but none sufficiently damaging enough to trigger the replacement of damaged components with low-damage equivalents. The final case in Figure 3(d) shows an initial moderate earthquake after 22 years, which is sufficiently strong to trigger the replacement of damaged components with new low-damage equivalents. In subsequent earthquakes, the losses in the low-damage repair case are less than the losses in the benchmark case. This is a clear indication of the benefits to be gained by replacing the damaged non-structural components with more resilient equivalents, as opposed to replacing them with identically vulnerable components following each major event.

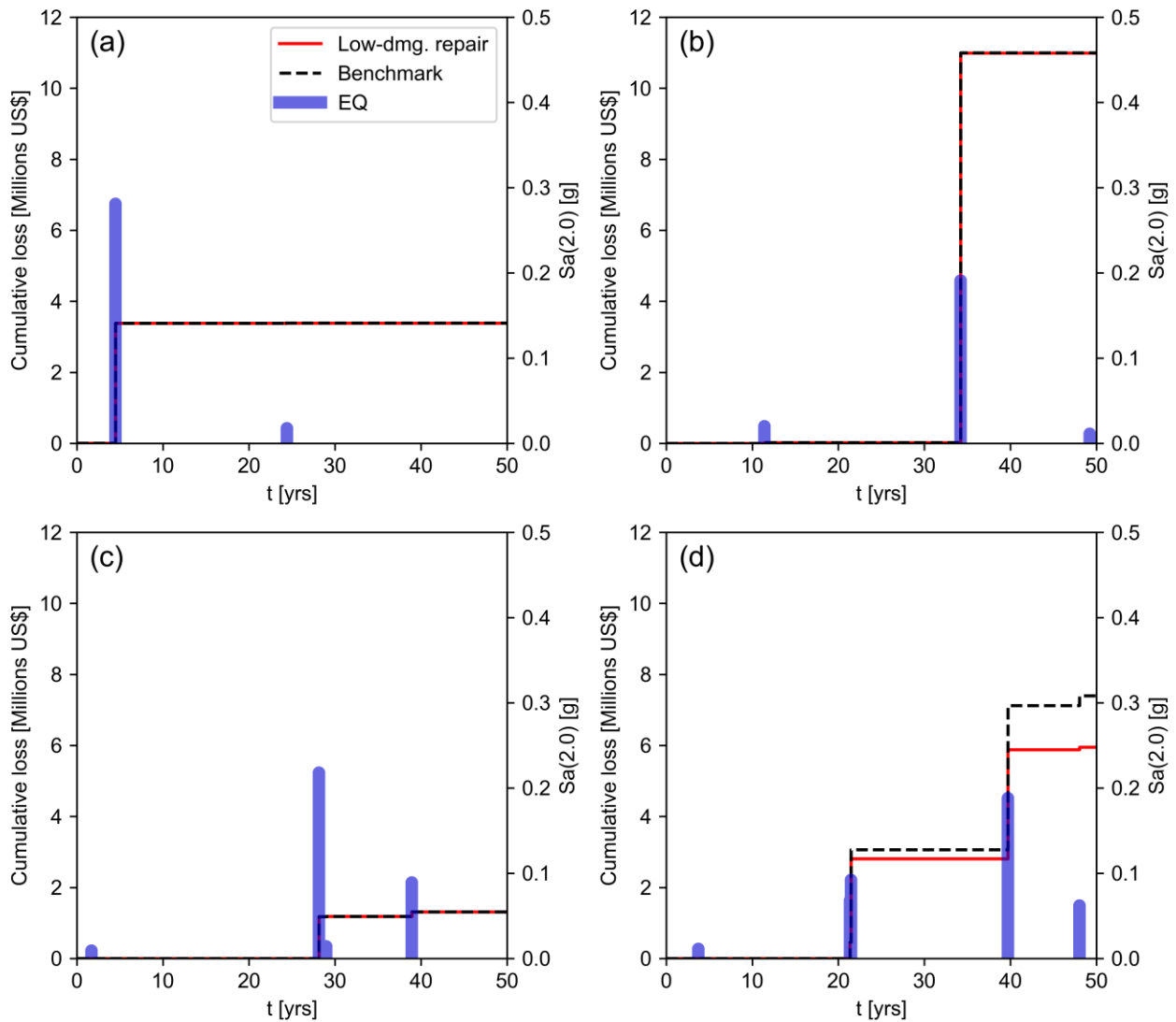


Figure 3. Cumulative losses in individual 50-year period simulations for the benchmark and low-damage repair cases.

#### 4.2. Results for all 50-year periods

Although it is informative to look at individual 50-year periods to understand how losses might progress, to inform decision-making, it is necessary to look at the outcomes from a large number of trials. Figure 4(a) shows a direct comparison of losses for the benchmark and low-damage repair cases for all cases examined. It can be observed that in a larger number of cases, the 50-year loss for the low-damage repair case is less than the loss for the benchmark case. The difference gets more significant as losses increase, for reasons explained in the previous section.

Figure 4(b) shows the empirical distribution function of 50-year losses for both cases. At the plotting scale that shows the full range of losses, it is difficult to visually observe differences between the two cases; however, it is still useful to observe that the vast majority of cases result in 50-year losses that are either very small or zero. In fact, from the 1000 total trials, 125 resulted in zero loss, while another 389 resulted in losses that were less than US\$100,000. As mentioned previously, the results of interest tend to be for the cases of large losses. Therefore, Figure 4(c) shows the same empirical cumulative distribution but only for losses greater than US\$4 million. In this range, it can be seen that there is a notable difference between the two distributions. A “jump” in the curves can also be observed at a loss of around US\$20 million, which corresponds to the replacement cost of the building, and therefore any trials exceeding this value almost certainly include instances of collapse.

An alternative approach to examine the difference between the two cases is to look at the EAL, which can be calculated as the sum of losses from all trials divided by the number of trials and the time period (50 years in this case). For the benchmark case, the EAL is US\$32,400, while for the low-damage replacement case, it is US\$30,500, which corresponds to a reduction of 6%.

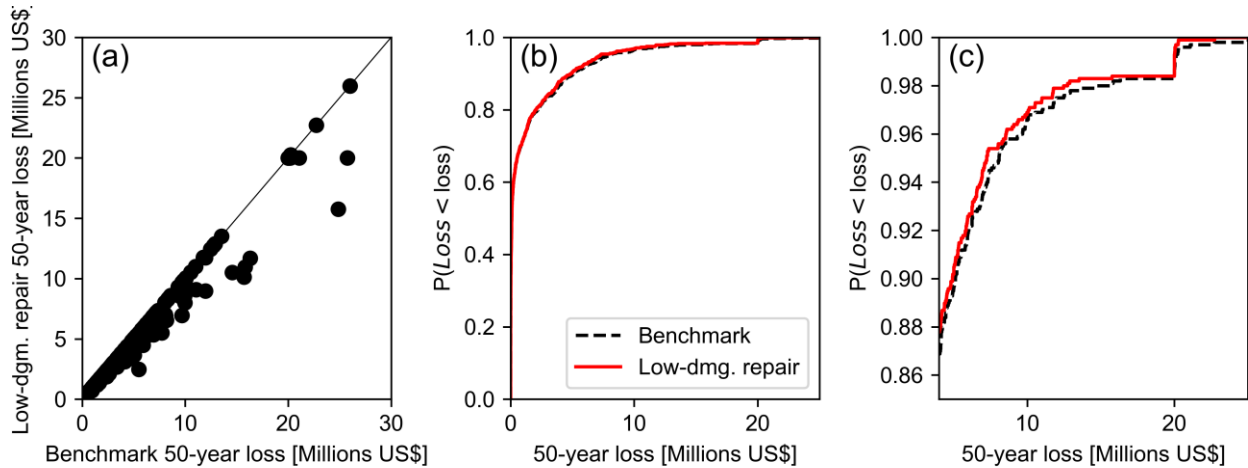


Figure 4. (a) Direct comparison of 50-year losses for the benchmark and low-damage repair cases. (b) Empirical cumulative distribution function of 50-year losses for both cases. (c) Empirical cumulative distribution function showing only the losses greater than US\$4 million.

## 5. Concluding remarks

This work has developed a methodology, based on FEMA P-58, for performing seismic loss assessment considering improvements of non-structural components during post-earthquake repairs. The methodology was then applied to a case-study 12-storey steel frame building hypothetically located in Wellington, New Zealand.

The results have shown that consideration of post-earthquake improvements will lead to a reduction in estimated loss (assuming there is no difference in the cost of conventional and low-damage components). For the case-study building, the difference in terms of EAL was 6%; however, this would be expected to vary significantly depending on the fragility of the as-built non-structural components, seismic response of the structure and local seismic hazard. Nevertheless, it is something that should be taken into account when considering the reduction of direct economic losses as a driver for the retrofit of non-structural components.

The change of state of a building over time and the post-earthquake decision-making process are both far more complex than has been considered in this simplified example. Future work could continue to develop the proposed methodology to consider some of these additional complexities, such as aftershocks, degradation of the structural system and non-seismic factors influencing the non-structural fit-out (e.g. intervention for energy efficiency improvements).

## 6. References

- Bradley B.A. (2010). A generalized conditional intensity measure approach and holistic ground motion selection, *Earthquake Engineering & Structural Dynamics*, 39(12):1324–1342.
- Bradley B.A. (2012). A ground motion selection algorithm based on the generalized conditional intensity measure approach, *Soil Dynamics & Earthquake Engineering*, 40:48–61.
- Carr A.J. (2004). *Ruaumoko 2D—inelastic dynamic analysis program*, Department of Civil and Natural Resources Engineering, University of Canterbury, Christchurch.
- Fox M.J., Yeow T.Z., Keen J.M., Sullivan T.J., Pavese A. (2024) New Zealand specific consequence functions for seismic loss assessment, *Bulletin of the New Zealand Society for Earthquake Engineering* (in press).



- Hamburger R.O. (1996). Implementing Performance Based Seismic Design in structural engineering practice, *Proceedings of the 11<sup>th</sup> World Conference on Earthquake Engineering*, Acapulco, Mexico.
- Iervolino I., Giorgi M., Chioccarelli E. (2016). Markovian modelling of seismic damage accumulation, *Earthquake Engineering & Structural Dynamics*, 45(3): 441–461.
- Retamales R., Davies R., Mosqueda G., Filiatrault A. (2013). Experimental seismic fragility of cold-formed steel framed gypsum partition walls, *Journal of Structural Engineering*, 139(8): 1285-1293.
- SNZ (1997). *NZS3404 Steel Structures Standard*, Standards New Zealand, Wellington.
- SNZ (2004). *NZS1170.5 Structural design actions Part 5 Earthquake actions – New Zealand*, Standards New Zealand, Wellington.
- Sousa L., Monteiro R. (2018). Seismic retrofit options for non-structural building partition walls: Impact on loss estimation and cost-benefit analysis, *Engineering Structures*, 161: 8–27.
- Yeow T.Z., Orumiyehi A., Sullivan T.J., MacRae G.A., Clifton G.C., Elwood K.J. (2018). Seismic performance of steel friction connections considering direct-repair costs, *Bulletin of Earthquake Engineering*, 16: 5963-5993.
- Yeow T.Z., Sullivan T.J., Elwood K.J. (2018). Evaluation of fragility functions with potential relevance for use in New Zealand, *Bulletin of the New Zealand Society for Earthquake Engineering*, 51(3): 127–144.

Table A1. Fragilities and unit repair costs for damageable structural and non-structural components

Original components										
Reference or NISTIR Classification	Component Name	θ			β			Unit repair cost [USD]		
		DS1	DS2	DS3	DS1	DS2	DS3	DS1	DS2	DS3
B1035.001	RBS connection 1-sided, beam depth <= W27	0.03	0.04	0.05	0.3	0.3	0.3	16033	25933	25933
B1035.011	RBS connection 2-sided, beam depth <= W27	0.03	0.04	0.05	0.3	0.3	0.3	26567	47000	47000
B1035.002	RBS connection 1-sided, beam depth >= W30	0.03	0.04	0.05	0.3	0.3	0.3	17033	28433	28433
B1035.012	RBS connection 2-sided, beam depth >= W30	0.03	0.04	0.05	0.3	0.3	0.3	28733	52399	52399
B1031.011b	Steel Column Base Plates	0.04	0.07	0.1	0.4	0.4	0.4	0	29395	36657
Retemales_Full	Partition wall full height	0.0027	0.0061	0.012	0.45	0.42	0.59	1803	4297	8991
Retemales_Part.	Partition wall partial height	0.0074	0.01	0.0179	0.29	0.33	0.28	1803	4297	8991
B2023.001	Generic Storefront	0.029	0.0473	0.07	0.5	0.25	0.25	935	1550	1550
B2022.032	Midrise stick-built curtain wall	0.0088	0.0108		0.25	0.25		1555	1555	
C2011.011b	Precast stair assembly	0.005	0.017	0.028	0.6	0.6	0.45	614	3711	23217
C3032.001d	Suspended Ceiling	0.56	1.08	1.31	0.25	0.25	0.25	3542	27633	59678
D1014.011	Traction Elevator	0.39			0.45			18133		
D2021.011b	Cold or Hot Potable	1.5	2.6		0.4	0.4		380	3800	
D2031.021b	Sanitary Waste Piping	1.2	2.4		0.5	0.5		423	3500	
D3031.013h	Chiller	1			0.72			263967		
D3031.022h	Cooling Tower	0.97			0.6			134657		
D3041.001a	HVAC Fan	1.92	2.4		0.5	0.5		7343	27702	
D3041.011c	HVAC Ductin	1.5	2.25		0.4	0.4		681	6464	
D3041.032c	HVAC Drops / Diffusers	1.5			0.4			2833		
D3041.041b	VAV box	1.9			0.4			14796		
D4011.021a	Fire Sprinkler Water Piping	1.1	2.4		0.4	0.5		348	2597	
D4011.031a	Fire Sprinkler Drop	0.75	0.95		0.4	0.4		526	526	
D5011.013h	Transformer/primary service	3.05			0.5			44351		
D3052.013b	Air Handling Unit	1.54			0.6			1053		
D2021.011a	Cold or Hot Potable Piping	1.5	2.6		0.4	0.4		290	2650	
D2031.021a	Sanitary Waste Piping	2.25			0.5			3167		
Replacement low-damage components										
Reference or NISTIR Classification	Component Name	θ			β			Unit repair cost [USD]		
		DS1	DS2	DS3	DS1	DS2	DS3	DS1	DS2	DS3
Retemales_Full (Improved)	Partition wall full height	0.0127	0.0161	0.022	0.45	0.42	0.59	1803	4297	8991
Retemales_Partial (Improved)	Partition wall partial height	0.0174	0.02	0.0279	0.29	0.33	0.28	1803	4297	8991
B2023.0022	Generic Storefront	0.0423	0.059	0.0665	0.3	0.25	0.35	935	1550	1550
B2022.022	Midrise stick-built curtain wall	0.0392	0.0434		0.29	0.25		1555	1555	
C3032.004d	Suspended Ceiling	1.31	2.03	2.29	0.3	0.3	0.3	3542	27633	59678
D2021.013b	Cold or Hot Potable	1.5			0.4			380		
D2031.024b	Sanitary Waste Piping	2.25			0.5			423		
D3041.001c	HVAC Fan	2.25	2.6		0.4	0.4		7343	27702	
D4011.024a	Fire Sprinkler Water Piping	1.9	3.4		0.4	0.4		348	2597	
D4011.034a	Fire Sprinkler Drop Standard Threaded Steel	1.3			0.4			526		
D2021.013a	Cold or Hot Potable Piping	2.25	4.1		0.4	0.4		290	2650	
D2031.024a	Sanitary Waste Piping	3			0.5			3167		